# The Mercury Isotopic Composition of Earth's Mantle and the Use of Mass Independently Fractionated Hg to Test for Recycled Crust

Frederic Moynier, Matthew G Jackson, Ke Zhang, Hongming Cai, Saemundur Ari Halldórsson, Raphael Pik, James M D Day, Jiubin Chen

# The Mercury Isotopic Composition of Earth's Mantle and the Use of Mass Independently Fractionated Hg to Test for Recycled Crust

**Frédéric Moynier[1,2*], Matthew G. Jackson[3], Ke Zhang[4], Hongming Cai[4], Sæmundur Ari Halldórsson[5], Raphael Pik[6], James M.D. Day[7], Jiubin Chen[2,4*]**

[1]Université de Paris, Institut de Physique du Globe de Paris, CNRS, 1 rue Jussieu, Paris 75005, France

[2]State Key Laboratory of Geological Processes and Mineral Resources, School of Earth Sciences, China University of Geosciences, Wuhan 430074, China

[3]Department of Earth Science, University of California, Santa Barbara, CA 93106

[4]Institute of Surface-Earth System Science, Tianjin University

[5]Nordic Volcanological Center, Institute of Earth Sciences, University of Iceland, Reykjavík, Iceland.

[6]Centre de Recherche Pétrographique et Géochimique, CNRS, Université de Lorraine, Nancy.

[7]Scripps Institution of Oceanography, University of California San Diego, La Jolla, CA 92093-0244, USA

*****Corresponding authors:

Corresponding authors: Frederic Moynier (moynier@ipgp.fr) and Jiubin Chen (jbchen@tju.edu.cn)

## Key Points:

- The Hg isotopic composition of the primitive mantle determined by analysing lavas from the Samoa and Iceland hotspots
- Key samples from the canonical mantle endmember analyzed to track crustal recycling in the mantle.
- We demonstrate the presence of recycled oceanic and continental materials in the source of ocean island basalts.

## Abstract

**The element mercury (Hg) can develop large mass-independent fractionation (MIF) ($\Delta^{199}$Hg) due to photo-chemical reactions at Earth's surface. This results in globally negative $\Delta^{199}$Hg for terrestrial sub-aerially-derived materials and positive $\Delta^{199}$Hg for sub-aqueously-derived marine sediments. The mantle composition least affected by crustal recycling is estimated from high-$^{3}$He/$^{4}$He lavas from Samoa and Iceland, providing an average of $\Delta^{199}$Hg=0.00±0.10, $\Delta^{201}$Hg=-0.02±0.0.09, $\delta^{202}$Hg=-1.7±1.2; 2SD, N=11. By comparison, a HIMU-type lava from Tubuai exhibits positive $\Delta^{199}$Hg, consistent with altered oceanic crust in its mantle source. A Samoan (EM2) lava has negative $\Delta^{199}$Hg reflecting incorporation of continental crust materials into its source. Three Pitcairn lavas exhibit positive $\Delta^{199}$Hg which correlate with $^{87}$Sr/$^{86}$Sr, consistent with variable proportions of continental (low $\Delta^{199}$Hg and high $^{87}$Sr/$^{86}$Sr) and oceanic (high $\Delta^{199}$Hg and low $^{87}$Sr/$^{86}$Sr) crustal material in their mantle sources. These observations indicate that MIF signatures offer a powerful tool for examining atmosphere-deep Earth interactions.**


## Plain language summary:

**While Earth's mantle is continuously chemically and isotopically stirred by convection, some ocean island lavas preserve isotopic anomalies. Their most likely origin is the recycling of crustal material into Earth's mantle by subduction. A question is then whether these crustal materials originate from the ocean or the continents. By using mercury stable isotopic compositions, which have specific signatures in ocean and continent materials, we identify whether these anomalies are due to continental or oceanic crustal material in various ocean island basalts.**

## 1 Introduction

The composition of Earth's mantle is in part known through the chemical and isotopic analyses of lavas from different tectonic settings such as mid-ocean ridge basalts (MORB) and ocean island basalts (OIB) [e.g. Hofmann, 2013]. The variable isotopic compositions of OIB are usually interpreted to reflect mantle heterogeneity formed by recycling of surface material back into the mantle through subduction, the contribution of Earth's core into the deep source of certain lavas, or the survival of early-formed heterogeneities in the mantle [e.g. Hauri and Hart, 1993; Hofmann, 1997; Hofmann and White, 1982; Mukhopadhyay and Parai, 2019; Mundl-Petermeier et al., 2020; Rizo et al., 2019]. Identifying the geological origin of such mantle sources is paramount to understand mantle dynamics through time.

Mantle heterogeneities have been defined and traditionally traced by using radiogenic isotopes such as Sr, Nd, Hf and Pb [e.g. Blichert-Toft et al., 1999; Blichert-Toft et al., 2003; Chauvel et al., 1992; Hofmann, 1988; 1997; White and Hofmann, 1982; Zindler and Hart, 1986], and several end-members have been defined : EM-1 (Enriched-Mantle 1, intermediate $^{87}Sr/^{86}Sr$ and low $^{206}Pb/^{204}Pb$), EM-2 (Enriched-Mantle 2, high $^{87}Sr/^{86}Sr$ and intermediate $^{206}Pb/^{204}Pb$), and HIMU (defined by low $^{87}Sr/^{86}Sr$ and high $^{206}Pb/^{204}Pb$). There is a general consensus emerging for the origin of EM-2 from continental crust materials (e.g. Jackson et al., 2007; White and Hofmann, 1982) and HIMU as oceanic crust and lithosphere or marine carbonates (e.g. Cabral et al., 2013; Chauvel et al., 1992; Hofmann and White, 1982), but the origin of EM-1 is debated (e.g. continental crust, pelagic sediments, delaminated sub-continental lithosphere or a common origin with EM-2 as terrestrial sediments; Castillo, 2017; Delavault et al., 2016; Eisele et al., 2012; Garapic et al., 2015) and understanding its origin represents an important challenge. Stable

isotope systems can give complementary information to radiogenic systems, but the potential sources of isotopic fractionation are diverse (e.g. magmatic differentiation, surficial processes), and their interpretation can be somewhat ambiguous.

A few stable isotope systems, the most notable being S, O and Hg, exhibit mass-independent isotopic fractionations (MIF) in naturally-occurring mantle-derived samples that are not strongly modified by high temperature processes [e.g. Cabral et al., 2013; Delavault et al., 2016; Moynier et al., 2020]. For example, the presence of MIF sulfur in Mangaia (Cook Islands, Polynesia) and Pitcairn lavas demonstrated the presence of an Archean atmosphere-derived sulfur component in their mantle source [Cabral et al., 2013; Delavault et al., 2016]. Mercury is the most volatile among the moderately volatile elements [Lodders, 2013] and exhibits large mass-dependent isotopic fractionations (MDF) and MIF. The MIF-Hg signatures of odd isotopes (odd-MIF) are due to magnetic isotope effects [e.g. Bergquist and Blum, 2007], or a nuclear field shift effect [Estrade et al., 2009] in surficial environments [e.g. Bergquist and Blum, 2007; Blum et al., 2013; Chen et al., 2012; Estrade et al., 2010; Foucher and Hintelmann, 2006; Sherman et al., 2010; Sonke et al., 2010], producing > ‰ effects. High temperature processes such as magmatic degassing produce limited (<10ppm) Hg-MIF [Moynier et al., 2020].

Mercury isotopes are mass-independently fractionated in surface samples and exhibit specific signatures related to different environments, showing potential application to study the nature of recycled materials in the mantle sources of lavas. This is due to the distinct MIF signatures of terrestrial surface environments whereby sub-aerially formed terrestrial reservoirs having generally negative odd-isotopes MIF [e.g. Blum et al., 2014] while the oceanic environment, including sediments and seawater, shows positive odd-isotope MIF [Meng et al., 2020; Meng et al., 2019; Yin et al., 2015]. In particular, it may be possible to test whether EM1 lavas sample a

component of deeply recycled terrestrial sediments [Castillo, 2017; Eisele et al., 2012; Garapic et al., 2015].

A recent landmark study showed that Hg from gold deposits associated with arc magmatism had positive odd-isotope MIF associated with recycling of marine Hg from the subduction zone into the mantle source of arc lavas [Deng et al., 2020]. This highlights the utility for Hg isotopes to serve as a tracer of deep recycling processes, from subduction zones to hotspots. Here, we test the origin of the material present in various end-member signatures (EM1, EM2, and HIMU) of OIB using Hg isotopes.

Due to the high volatility of mercury, constraints on its isotopic composition within Earth's mantle are critical for evaluating the origin of terrestrial volatile elements by means of comparison with the isotopic composition of primitive meteorites [Meier et al., 2016; Moynier et al., 2020]. However, the Hg isotopic composition of the mantle has been estimated from only four basaltic rocks [Geng et al., 2018; Moynier et al., 2020], and these samples may not be ideally suited for evaluating the composition of the primitive mantle. A primary hurdle for Hg isotopic characterization of mantle-derived lavas is their low Hg contents (a few ppb). We have recently developed a method that yields high precision data on less than 5ng of Hg, which enables isotope characterization with just a few grams of material [Moynier et al., 2020]. This allows targeting of a key set of mantle-derived lavas to evaluate the Hg isotopic composition of the mantle least impacted by crustal recycling, and place key constraints on the origin of the volatile element Hg on Earth.

To evaluate the Hg isotopic composition of the mantle least affected by crustal recycling, we selected lavas with least degassed signatures reflected by their high-$^{3}He/^{4}He$ (>13 atmospheric

ratio, $R_A$), including four samples from Samoa [Jackson et al., 2007], and seven from Iceland [Füri et al. 2010 and Halldórsson et al. 2016b]. To further characterize the composition of the mantle we analysed three additional Icelandic samples [Óskarsson et al. 1982] and six basalts from the Afar (Ethiopia) [Deng et al., 2018; Pik et al., 2006]. To search for deep recycling of surface-derived Hg, samples from the three canonical mantle endmembers thought to reflect deep recycling of crustal materials: EM1 (Pitcairn, N=3), HIMU (Tubuai, N=1), EM2 (Samoa, N=1) were selected.

## 2 Materials and Methods

### 2.1 Sample descriptions

We report isotopic data on international rock standards to assess data quality and intra-laboratory data comparisons: USGS samples: BCR-2 (basalt, USA), RGM-2 (Rhyolite, USA) and STM-2 (syenite, USA) and three Icelandic samples used as internal standards at the University of Iceland (I-ICE, A-ALK, B-ALK, Óskarsson et al. 1982), all of which are available upon request. The Hg isotopic composition of BCR-2 has been reported previously [Geng et al., 2018]. One trachyandesite from the Samoa hotspot (ALIA-115-21) [Adams et al., 2021], three basalt samples from Pitcairn [Garapic et al., 2015], and one basalt sample from Tubuai [Hauri and Hart, 1993] were selected to represent the EM2, EM1 and HIMU mantle end-members, respectively. Four samples from Ofu island (Samoa [Jackson et al., 2007]) and seven samples from several different regions (Eastern Rift Zone, Reykjanes Peninsula, Western Rift Zone, and Northern Rift Zone) of Iceland [Halldórsson et al., 2016ab; Jackson et al., 2020; Macpherson et al., 2005; Rasmussen et al., 2019] were taken to represent the high-$^3He/^4He$ mantle (>13$R_A$). Six basalt samples from the Stratoid Series in the Afar hotspot [Deng et al., 2018; Pik et al., 2006] were

selected to further estimate the mantle composition. While the $^{3}He/^{4}He$ of the Afar samples have not been characterized, the composition of samples from this region is ~10-13 $R_A$ [Marty et al., 1996; Medynsky et al., 2013]. The UM-Almedén cinnabar standard was also analysed for inter-laboratory comparison.

## 2.2 Methods

The method follows the same protocol as in Moynier et al. [2020]. The Hg isotopic analysis was carried out using a MC-ICP-MS (Nu-Plasma-3D, Nu-Instruments) [Chen et al., 2010; Huang et al., 2015; Yuan et al., 2018; Zhang et al., 2020]. The instrumental mass bias was corrected by an internal NIST-SRM-997-Tl standard using the standard-sample bracketing method. All samples were analyzed in three blocks (33 cycles). A 10-minute washout time in between samples

149 ensured blank levels <0.2% of the preceding sample signals. Signal intensities were 2.5V on
150 $^{202}Hg$ (1 ppb solution).

151 The data for Hg-MDF is reported as $\delta^{x}Hg$ :

152 $$\delta^{x}Hg\ (‰)=[(^{x}Hg/^{198}Hg)_{sample}/(^{x}Hg/^{198}Hg)_{NIST\ SRM\ 3133}-1]\times 1000 \quad \text{(Eq. 1)}$$

153 where x refers to 199, 200, 201, or 202. $\delta^{202}Hg$ is used for the discussion of MDF. The MIF data
154 are defined as the deviation of the $\delta^{x}Hg$ from the theoretical value based on kinetic isotopic
155 fractionation [e.g. Blum and Johnson, 2017]:

156 $$\Delta^{x}Hg(‰)=\delta^{x}Hg(‰)-\beta^{x}\times\delta^{202}Hg \quad \text{(Eq. 2)}$$

157 where the mass dependent scaling factor $\beta^{x}$ is 0.2520, 0.5024 and 0.7520 for $^{199}Hg$, $^{200}Hg$ and
158 $^{201}Hg$, respectively.

159 Errors are reported as twice the standard deviation from the replicates of the same solution, and
160 are typically 0.08‰, 0.03‰, 0.03‰, 0.05‰ for $\delta^{202}Hg$, $\Delta^{199}Hg$, $\Delta^{200}Hg$ and $\Delta^{201}Hg$,
161 respectively. Long-term measurements of UM-Almadén Hg and CRM-GBW07405 standards
162 give identical values for Hg isotopic composition (both MDF and MIF) to literature [Chen et al.
163 2010; Moynier et al. 2020; Huang et al. 2019], attesting the quality of Hg isotope analysis.

164 **3 Results**

165 Isotopic data for samples are reported in Table S1 and the $\Delta^{199}Hg$ values are reported
166 against $\delta^{202}Hg$ values in Figure 1. The isotopic composition of BCR-2 is identical within error to
167 literature values [Geng et al., 2018].

168 The terrestrial igneous rock samples show variable $\delta^{202}$Hg values, from -3.23 to -0.01,
169 consistent with literature data [Geng et al., 2018; Moynier et al., 2020] (Figure 1). High $^{3}$He/$^{4}$He
170 localities - Ofu island and Iceland- do not exhibit any MIF, and the Afar samples also lack MIF-
171 Hg signatures. By contrast, the HIMU sample from Tubuai has a positive odd-isotope-MIF
172 ($\Delta^{199}$Hg=+0.23±0.07). The extreme EM2 Samoa ALIA-115-21 sample has a distinct negative odd-
173 isotope-MIF signature ($\Delta^{199}$Hg=-0.14±0.02). In the Pitcairn lava suite, there is a positive
174 correlation between $^{87}$Sr/$^{86}$Sr and MIF-Hg: two Pitcairn lavas with the less extreme EM1 signatures
175 have clear negative odd-isotope-MIF-Hg ($\Delta^{199}$Hg down to -0.45±0.01), while the Pitcairn sample
176 with the most extreme EM1 signature has no resolvable MIF (Figure 2). No samples exhibit even-
177 isotope-MIF signatures.

178 **4.Discussion**

179 **4.1 The isotopic composition of the primitive mantle.**

180 Before discussing the potential effects of recycling of surficial material on the Hg isotopic
181 composition of mantle sources, it is critical to establish the composition of the primitive mantle.
182 OIB with the highest $^{3}$He/$^{4}$He are inferred to sample mantle sources that are least degassed [Craig
183 and Lupton, 1976; Mukhopadhyay and Parai, 2019] and the least modified by crustal recycling
184 [Jackson et al., 2020; White, 2015]. Making the assumption that these samples represent materials
185 with Hg isotopic compositions consistent with the most "pristine" mantle domain, we can then
186 establish the impact of crustal subduction and recycling on the Hg systematics of mantle-derived
187 lavas.

188 The Ofu island samples have high-$^{3}$He/$^{4}$He (22$R_A$ to 34$R_A$, see Table S1) [Jackson et al.,
189 2007] and are inferred to sample an ancient mantle domain [Mundl-Petermeier et al., 2020] less
190 impacted by crustal recycling than other Samoan lavas [Jackson et al., 2020]. Given that the high-

$^{3}He/^{4}He$ reservoir is least impacted by recycling, and the discovery that some high-$^{3}He/^{4}He$ lavas preserve early-Hadean signatures identified using several different short-lived isotope systems - $^{129}Xe/^{130}Xe$ [Mukhopadhyay and Parai, 2019], $^{142}Nd/^{144}Nd$ [Peters et al., 2018], and $^{182}W/^{184}W$ [Mundl-Petermeier et al., 2020; Rizo et al., 2019]-this mantle reservoir is most likely to preserve signatures associated with terrestrial accretion. Indeed, arguments have been made that the high-$^{3}He/^{4}He$ reservoir is the oldest domain that has survived in Earth's mantle [Giuliani et al., 2020; Jackson et al., 2010] but alternative views exist [e.g. Mukhopadhyay and Parai, 2019]. Therefore, the absence of Hg-MIF in the high-$^{3}He/^{4}He$ samples suggests that Earth's mantle accreted Hg devoid of MIF, and therefore any observed MIF are the consequence of terrestrial fractionation. Combining Hg isotope data from the Ofu (N=4) with Iceland samples for which $^{3}He/^{4}He$ are available (N=7, all of which have $13<^{3}He/^{4}He<34$), return an average Hg isotopic composition for the mantle of $\Delta^{199}Hg=0.00\pm0.10$ and $\Delta^{201}Hg=-0.02\pm0.0.09$ (2SD, N=11). This represents the current best estimate of the terrestrial "primitive mantle" composition. The $\delta^{202}Hg$ values are more variable within these samples. Since Hg is highly volatile, degassing during magma ascent can induce isotopic fractionation [e.g. Zambardi et al. 2009], and further isotopic fractionation could also occur during igneous processes. Therefore, compared to MIF-Hg signatures, which should not be significantly impacted by high temperature magmatic and degassing processes, the $\delta^{202}Hg$ values are likely more impacted by the processes leading to the formation of the basalts. Nevertheless, the $\delta^{202}Hg$ of the 11 high-$^{3}He/^{4}He$ samples from Ofu island and Iceland show limited variation, with an average $-1.7\pm1.2$ (2SD, N=11), which compare well with a previous estimate of the mantle composition based on only a few unrelated igneous rocks ($\delta^{202}Hg$ <-2.35, [Moynier et al., 2020], see Figure S1). Furthermore, samples from the Afar ($^{3}He/^{4}He$ ~10-13 Ra, [Marty et al.,

1996; Medynsky et al., 2013]) (N=6) have similar Hg isotopic composition within error, suggesting a large-scale homogeneity of Earth's modern mantle.

Our estimate of the primitive mantle Hg isotopic composition falls within the range defined by chondrites (Figure 3). While the large uncertainties on the Hg concentration of the Earth's mantle prevent an accurate estimate the amount of terrestrial Hg that is stored into the Earth's core, the present chondritic isotopic composition of the Earth's primitive mantle is an argument that late accretion of chondritic material delivered the present mantle Hg (and other volatile elements) (see discussion in Moynier et al. [2020]). This conclusion is consistent with observations made from C, N and noble gas isotopes [Marty, 2012] and the volatile and chalcophile elements S, Se and Te [Wang and Becker 2013; Varas-Reus et al. 2019].

### 4.2. Evidence for Hg recycling?

Considering the Hg isotopic composition of high-$^{3}He/^{4}He$ lavas defined above as representative of the mantle domains the least modified by crustal recycling, we can compare our estimate for the Hg isotopic composition for low-$^{3}He/^{4}He$ mantle endmembers that are suggested to host recycled surface materials—EM1 Pitcairn (EM1), Samoa (EM2), and Tubuai (HIMU)—and then identify Hg isotope signatures associated with recycling in the mantle sources of these lavas.

Three OIB samples examined in this study that represent mantle end-member compositions— TBA-B3 (Tubuai HIMU), ALIA-115-21 (Samoa EM2), and two Pitcairn lavas (Pit-6 and Pit-8)—show clearly resolvable odd-MIF. The correlation between $\Delta^{199}Hg$ and $\Delta^{201}Hg$ values with a slope of ~1 (Figure 4), typical of surface photochemical reactions on Hg [Bergquist and Blum, 2007], suggests that the three samples share likely a similar origin for the MIF signatures in surficial environments. The Hg-MIF signatures in OIB therefore provides evidence

for recycling of shallow geochemical reservoirs into the deep sources of hotspots. This correlation between $\Delta^{199}$Hg and $\Delta^{201}$Hg values also provides further confidence on the quality of the data as isobaric interference would produce isotopic signatures that lie outside of this range.

Photochemical reduction of aqueous Hg(II) to Hg(0) vapor is the major source of odd-MIF, and is the main pathway of transfer of Hg from the ocean (surface) to the atmosphere [e.g. Bergquist and Blum, 2007]. During the photochemical reduction, a positive $\Delta^{199}$Hg [Hg(II)] is retained in the marine environment while the complementary negative $\Delta^{199}$Hg [Hg(0)] is released into the atmosphere [e.g. Bergquist and Blum, 2007]. Given the short residence time of Hg(0) in the atmosphere (~1 year), its quick subsequent deposition confers a globally negative $\Delta^{199}$Hg to the terrestrial reservoirs, while marine environments are characterized by positive $\Delta^{199}$Hg [e.g. Biswas et al., 2008; Blum et al., 2014; Demers et al., 2015; Grasby et al., 2017; Jiskra et al., 2017]. How a negative $\Delta^{199}$Hg preserved in terrestrial material is then transported into the ocean through time is unclear at present. Further work is required to test the robustness of this negative signature on long timescales necessary for this material to be recyclied within the mantle. This difference between terrestrial and marine settings is well reflected in sediments, with generally negative $\Delta^{199}$Hg in coastal sediments (which originate via erosion of nearby terrestrial materials) and positive $\Delta^{199}$Hg for open sea marine sediments [e.g. Meng et al., 2019; Yin et al., 2015]. The odd-MIF of ALIA-115-21 (Samoa EM2), TBA-B3 (Tubuai HIMU), and Pit-6 and Pit-8 (Pitcairn) therefore likely reflect a marine Hg isotopic signature in Tubuai, and continental Hg signatures Samoan EM2 lavas (Figure 4). As discussed below, Pitcairn lavas exhibit Hg isotopic evidence for recycled marine and terrestrial materials.

The presence of marine and continental signatures in the mantle sources of Tubuai HIMU and Samoa EM2 lavas, respectively, is consistent with traditional interpretations based on radiogenic

isotope signatures. Tubuai exhibits a HIMU signature, which is considered to result from recycling of ancient oceanic crust into the mantle [Hofmann and White, 1982]. The geochemically-depleted $^{87}Sr/^{86}Sr$ and $^{143}Nd/^{144}Nd$ signatures in HIMU lavas globally precludes a significant sediment (terrigenous or marine) contribution to their mantle sources, but transfer of positive $\Delta^{199}Hg$ isotope compositions of seawater to oceanic crust during hydrothermal circulation at a mid-ocean ridge could explain the MIF signatures in Tubuai HIMU OIB. A potential caveat with this model is the low abundance of Hg in seawater compared to fresh basalts that would require a water/rock ratio of ~1000 to transfer the Hg isotopic composition of seawater to oceanic crust. However, the absence of data on Hg behavior during seawater alteration of oceanic crust (e.g., Hg concentration measurements on altered oceanic crust, including serpentinites) limits our ability to quantitatively model this scenario. An additional complexity is that a fraction of the slab Hg budget would be lost during subduction dehydration, but relevant data are not yet available to quantify this. By contrast, Samoan EM2 lavas exhibit geochemically-enriched (high)$^{87}Sr/^{86}Sr$ and (low) $^{143}Nd/^{144}Nd$ signatures consistent with the input of recycled terrigenous materials [Jackson et al., 2007; Workman et al., 2008], consistent with the slightly negative $\Delta^{199}Hg$ terrestrial signature.

The presence of negative $\Delta^{199}Hg$ in the source of Pitcairn EM1 OIB suggests that, like EM2, EM1 contains a fraction of recycled terrigenous material [Castillo, 2017; Delavault et al., 2016; Stracke, 2012]. However, there is complexity in the MIF present in the Pitcairn suite that is not explained by our simple model: the correlation between the $\Delta^{199}Hg$ and $^{87}Sr/^{86}Sr$ for the three Pitcairn samples (Figure 2) is puzzling, as we would expect the sample with the highest $^{87}Sr/^{86}Sr$ to host the largest fraction of continent-derived material and, therefore, the lowest $\Delta^{199}Hg$. Instead, the Pitcairn lava with the weakest EM1 signature has the strongest negative $\Delta^{199}Hg$, and the most extreme EM1 Pitcairn lava has no resolvable $\Delta^{199}Hg$ signature. The positive correlation between

282 $\Delta^{199}$Hg and $^{87}Sr/^{86}Sr$ is unlikely to be explained by seawater alteration, a mechanism that would
283 increase both $\Delta^{199}$Hg and $^{87}Sr/^{86}Sr$. This is because 1) $\Delta^{199}$Hg also exhibit a negative correlation
284 with $^{143}Nd/^{144}Nd$ (Figure S2), a radiogenic isotope system immune to seawater influence, and 2)
285 the selected Pitcairn lavas are young (<1.0Ma; [Duncan et al., 1974]) and fresh (i.e., no signs of
286 visible alteration). Therefore, we explore a mantle source origin for the correlation between
287 $^{87}Sr/^{86}Sr$ and $\Delta^{199}$Hg, acknowledging that this relationship is only for three samples.

288 Unlike Samoan EM2 (which is a melt of a peridotite mantle source that hosts recycled
289 terrigenous material) [Jackson and Shirey, 2011] and Tubuai HIMU (which is a melt of a
290 mantle source with recycled oceanic crust) [Hauri and Hart, 1993], extreme Pitcairn EM1 is
291 suggested to host both recycled oceanic crust and terrigenous materials [Eisele et al., 2003]. A
292 mixture of both recycled oceanic crust and terrigenous materials can help to explain the correlation
293 between $\Delta^{199}$Hg and $^{87}Sr/^{86}Sr$ (Figure 2), where Pitcairn's extreme EM1 endmember
294 (highest $^{87}Sr/^{86}Sr$) lacks a clear odd-MIF, and the Pitcairn lava with the weakest EM1 signature
295 (lowest $^{87}Sr/^{86}Sr$) has a negative $\Delta^{199}$Hg. Because recycled oceanic crust and terrigenous materials
296 have complementary positive and negative $\Delta^{199}$Hg signatures, respectively, it is possible for their
297 mixture to generate in a near-zero $\Delta^{199}$Hg value like that observed in the extreme Pitcairn EM1
298 sample. In this case, the presence of terrigenous materials explains the high $^{87}Sr/^{86}Sr$ in the extreme
299 EM1 Pitcairn lava. In contrast, the Pitcairn lava with the lowest $^{87}Sr/^{86}Sr$ (weakest EM1
300 signature) is explained by a smaller fraction of recycled terrigenous material, and the very negative
301 $\Delta^{199}$Hg in this lava can explained by the absence (or near absence) of oceanic crust (which would
302 have apositive $\Delta^{199}$Hg values): the remaining contribution of recycled terrigenous material has
303 strongly negative $\Delta^{199}$Hg, and explains the negative $\Delta^{199}$Hg values determined in lavas. In this
304 way, the relative proportions and absolute abundances of recycled terrigenous and oceanic crust

materials can be modulated to explain the magnitude and sign of the $\Delta^{199}$Hg values, and its relationship with radiogenic isotopes.

## 5. Conclusions

To estimate the Hg isotopic composition of the mantle that is least affected by crustal recycling, we analysed high-$^{3}$He/$^{4}$He lavas from Samoa and Iceland. We obtained an average $\Delta^{199}$Hg=0.00±0.10, $\Delta^{201}$Hg=-0.02±0.0.09 and $\delta^{202}$Hg=-1.7±1.2 (2SD, N=11), which is the best estimate for the composition of the primitive mantle.

HIMU lavas from Tubuai exhibit positive Hg-MIF, likely reflecting a transfer of the isotope compositions of seawater to oceanic crust during hydrothermal circulation at a mid-ocean ridge; positive Hg-MIF therefore signals the presence of altered oceanic crust in its mantle source. The negative MIF observed for EM2 lava from Samoa is consistent with assimilation of continental crust material. The negative MIF for the Pitcairn lavas, and the positive correlation of $\Delta^{199}$Hg values with $^{87}$Sr/$^{86}$Sr, provides an independent argument in favor of mixture between terrestrial and marine materials in the mantle source of EM1.

**Acknowledgments, Samples, and Data**

Runsheng Yin and Michael Bizimis are thanked for insightful reviews that have improved this manuscript. This study was supported by the National Natural Science Foundation of China (41625012, 41961144028, U1612442, 41830647) to JB.C and by the China National Space Administration (No. D020205) to ZW. FM thanks Yongsheng Liu for making the visit at CUG Wuhan possible. MGJ thanks IPGP for providing a stimulating academic home during sabbatical, and acknowledges partial support from NSF EAR-1900652 and OCE-1928970.

**Open Research section**

All the data are presently provided as a supplementary table and will be deposit on the CNRS HAL website as well as on the database Earthchem: https://earthchem.org/

## References:


Adams, J., J. M., F. Spera, A. Price, B. Byerly, G. Seward, and J. Cottle (2021), Extreme isotopic heterogeneity in Samoan clinopyroxenes constrains sediment recycling, Nature com., 12, 1234.

Bergquist, B. A., and J. D. Blum (2007), Mass-dependent and-independent fractionation of Hg isotopes by photoreduction in aquatic systems, Science, 318, 417-420.

Biswas, A., J. D. Blum, B. A. Bergquist, G. J. Keeler, and Z. Xie (2008), Natural mercury isotope variation in coal deposits and organic soils, Env. Sci. & Tech., 42, 8303-8309.

Blichert-Toft, J., F. A. Frey, and F. Albarède (1999), Hf isotope evidence for pelagic sediments in the source of Hawaiian basalts, Science, 285, 879-882.

Blichert-Toft, J., D. Weis, C. Maerschalk, A. Agranier, and F. Albarède (2003), Hawaiian hot spot dynamics as inferred from the Hf and Pb isotope evolution of Mauna Kea volcano, Geochem. Geophys. Geosyst., 4, doi:10.1029/2002GC000340.

Blum, J., and M. Johnson, W. (2017), Recent developments in mercury stable isotopes analysis, in Non-traditional stable isotopes, edited by F.-Z. Teng, J. Watkins and N. Dauphas, pp. 733-757, Mineralogical society of America.

Blum, J., B. Popp, J. Drazen, C. Choy, and M. Johnson (2013), Evidence for methylmercury production below the mixed layer in the central North Pacific Ocean, Nat. Geosci., 6, 879-884.

Blum, J., L. Sherman, and M. W. Johnson (2014), Mercury Isotopes in Earth and Environmental Sciences, A. Rev. Earth and Plane. Sci., 42, 249-269.

Cabral, R., M. Jackson, E. Rose-Koga, K. Koga, M. Whitehouse, M. Antonelli, J. Farquhar, J. Day, and E. Hauri (2013), Anomalous sulphur isotopes in plume lavas reveal deep mantle storage of Archaean crust, Nature, 496, 490-493.

Castillo, P. (2017), An alternative explanation for the Hf-Nd mantle array, Science Bulletin, 62, 974-975.

Chauvel, C., A. W. Hofmann, and P. Vidal (1992), HIMU-EM: The French Polynesian connection, Earth Planet. Sci. Lett., 110, 99-119.

Chen, J., H. Hintelmann, and B. Dimock (2010), Chromatographic pre-concentration of Hg from dilute aqueous solutions for isotopic measurement by MC-ICP-MS, J. Anal. Atom. Spec., 25, 1402-1409.

Chen, J., H. Hintelmann, X. Feng, and B. Dimock (2012), Unusual fractionation of both odd and even mercury isotopes in precipitation from Peterborough, ON, Canada, Geochim. Cosmochim. Acta, 90, 33-46.

Craig, H., and J. E. Lupton (1976), Primordial neon, helium, and hydrogen in oceanic basalts, Earth Planet. Sci. Lett., 31, 369-385.

Delavault, H., C. Chauvel, E. Thomassot, C. Devey, and B. Dazas (2016), Sulfur and lead isotopic evidence of relic Archean sediments in the Pitcairn mantle plume, Proc. Nat. Ac. Sci., 113, 12952-12956.

Demers, J. D., J. Blum, and D. Zac (2015), Mercury isotopes in a forested ecosystem: Implications for air-surface exchange dynamics and the global mercury cycle., Adv. Earth Space Sci. 27, 222-238.

Deng, C., G. Sun, Y. Rong, R. Sun, D. Sun, B. Lehmann, and R. S. Yin (2020), Recycling of mercury from the atmosphere-ocean system into volcanic arc associated epithermal gold systems. Geology, 49, 309–313.

Deng, Z., M. Chaussidon, P. Savage, F. Robert, R. Pik, and F. Moynier (2018), Titanium isotopes as a tracer for the plume or island arc affinity of felsic rocks, Proc. Nat. Ac. Sci., 116, 1132-1135.

Duncan, R., McDougall, I., Carter, R., Coombs, D., 1974. Pitcairn island— another Pacific hot spot? Nature 251, 619–682.

Eisele, J., W. Abouchami, S. J. G. Galer, and A. W. Hofmann (2003), The 320 kyr Pb isotope evolution of Mauna Kea lavas recorded in the HSDP-2 drill core, Geochem. Geophys. Geosyst., 4, doi: 10.1029/2002GC000339.

Eisele, J., M. Sharma, S. J. G. Galer, J. Blichert-Toft, C. Devey, and A. W. Hofmann (2012), The role of sediment recycling in EM-1 inferred from Os, Pb, Hf, Nd, Sr isotope and trace element systematics of the Pitcairn hotspot, Earth Planet. Sci. Lett., 196, 197-212.

Estrade, E., J. Carignan, J. E. Sonke, and O. Donard (2009), Mercury isotope fractionation during liquid-vapor evaporation experiments, Geochim. Cosmochim. Acta, 73, 2693-2711.

Estrade, N., J. Carignan, and O. Donard (2010), Isotope tracing of atmospheric mercury sources in an urban area of northeastern France, Environ. Sci. Technol., , 44, 6062-6067.

Foucher, D., and H. Hintelmann (2006), High-precision measurement of mercury isotope ratios in sediments using cold-vapor generation multi-collector inductively coupled plasma mass spectrometry, Anal. Bioanal. Chem., 384, 1470-1478.

Füri, E., D. Hilton, S. Halldórsson, P. Barry, D. Hahm, T. Fischer, and K. Grönvold (2010), Apparent decoupling of the He and Ne isotope systematics of the Icelandic mantle: The role of He depletion, melt mixing, degassing fractionation and air interaction, Geochim. Cosmochim. Acta, 74, 3307–3332.

Garapic, G., M. Jackson, E. Hauri, S. R. Hart, K. A. Farley, J. Blusztajn, and J. Woodhead (2015), A radiogenic isotopic (He-Sr-Nd-Pb-Os) study of lavas from the Pitcairn hotspot: Implications for the origin of EM-1 (enriched mantle 1), Lithos, 228, 1-11.

Geng, H., R. S. Yin, and X. Li (2018), An optimized protocol for high precision measurement of Hg isotopic compositions in samples with low concentrations of Hg using MC-ICP-MS, J. Anal. Atom. Spec, 33, 1932-1940.

Giuliani, A., M. G. Jackson, A. Fitzpyane, and H. Dalton (2020), Remnants of early Earth differentiation in the deepest mantle-derived lavas., Proc. Nat. Ac. Sci, 118, e2015211118.

Grasby, S. E., W. Shen, R. Yin, J. D. Gleason, J. D. Blum, and R. F. Lepak (2017), Isotopic signatures of mercury contamination in latest Permian oceans, Geology, 45, 55-58.

Halldórsson, S., J. Barnes, A. Stefánsson, D. Hilton, E. Hauri, and E. Marshall (2016a), Subducted lithosphere controls halogen enrichments in the Iceland mantle plume source, Geology, 44, 679-682.

Halldórsson, S., D. Hilton, P. Barry, E. Füri, and K. Grönvold (2016b), Recycling of crustal material by the Iceland mantle plume: new evidence from nitrogen elemental and isotope systematics of subglacial basalts, Geochim. Cosmochim. Acta, 176, 206-226.

411 Hauri, E. H., and S. R. Hart (1993), Re-Os isotope systematics of EMII and HIMU oceanic basalts
412 from the south Pacific Ocean, Earth Planet. Sci. Lett., 114, 353-371.
413 Hofmann, A. W. (1988), Chemical differentiation of the Earth: the relationship between mantle
414 continental crust, and oceanic crust, Earth Planet. Sci. Letters, 90, 297-314.
415 Hofmann, A. W. (1997), Mantle geochemistry: the message from oceanic volcanism, Nature,
416 385, 219-229.
417 Hofmann, A. W. (2013), Sampling Mantle Heterogeneity through Oceanic Basalts: Isotopes and
418 Trace Elements, in Treatise on Geochemistry, edited by H. D. Holland and K. K. Turekian, pp. 61-
419 101, Elsevier.
420 Hofmann, A. W., and W. M. White (1982), Mantle plumes from ancient oceanic crust, Earth
421 Planet. Sci. Lett., 57, 421-436.
422 Huang, Q., Y. Liu, J. Chen, X. Feng, W. Huang, S. Yuan, H. Cai, and X. Fu (2015), An improved
423 dual-stage protocol to pre-concentrate mercury from airborne particles for precise isotopic
424 measurement., J. Anal. Atom. Spectr. , 30, 957–966.
425 Huang, Q., Chen, J., Huang, W., Reinfelder, J.R., Fu, P., Yuan, S., Wang, Z., Yuan, W., Cai, H.,
426 Ren, H., 2019. Diel variation in mercury stable isotope ratios records photo-reduction of PM 2.5-
427 bound mercury. Atmos. Chem. Phys. 10, 315–325.
428 Jackson, M., S. R. Hart, A. Koppers, H. Staudigel, J. Konter, J. Blusztajn, M. Kurz, and J. Russell
429 (2007), The return of subducted continental crust in Samoan lavas, Nature 448, 684-687.
430 Jackson, M. G., et al. (2020), Ancient He and W isotopic signatures preserved in mantle domains
431 least modified by crustal recycling, PNAS, 117, 30993-31001.
432 Jackson, M. G., R. Carlson, M. Kurz, P. D. Kempton, D. Francis, and J. Blusztajn (2010), Evidence
433 for the survival of the oldest terrestrial mantle reservoir., Nature, 466, 853-856.
434 Jackson, M. G., and S. B. Shirey (2011), Re–Os isotope systematics in Samoan shield lavas and
435 the use of Os-isotopes in olivine phenocrysts to determine primary magmatic compositions,
436 Earth Planet. Sci. Lett., 312, 91-101.
437 Jiskra, M., J. G. Wiederhold, U. Skyllberg, R. M. Kronberg, and R. Kretzschmar (2017), Source
438 tracing of natural organic matter bound mercury in boreal forest runoff with mercury stable
439 isotopes, Environmental Science: Processes & Impacts, 19, 1235-1248.
440 Macpherson, C. C., D. Hilton, J. Day, D. Lowry, and K. Gronvold (2005), High-3He/4He, depleted
441 mantle and low d18O, recycled oceanic lithosphere in the source of central Iceland magmatism,
442 Earth Planet. Sci. Lett., 233, 411–427.
443 Marty, B. (2012), The origins and concentrations of water, carbon, nitrogen and noble gases on
444 Earth, Earth Planet. Sci. Lett., 314, 56-66.
445 Marty, B., R. Pik, and Y. Gezahegn (1996), Helium isotopic variations in Ethiopian plume lavas:
446 nature of magmatic sources and limit on lower mantle contribution, Earth Planet. Sci. Lett., 144,
447 223-237.
448 Medynsky, S., et al. (2013), Controlsonmagmaticcyclesanddevelopmentofrifttopographyofthe
449 Manda Hararosegment(Afar,Ethiopia):Insightsfromcosmogenic 3He
450 investigationoflandscapeevolution, Earth Planet. Sci. Lett., 367, 133-145.
451 Meier, M., C. Cloquet, and B. Marty (2016), Mercury (Hg) in meteorites: Variations in
452 abundance, thermal release profile, mass-dependent and mass-independent isotopic
453 fractionation, Geochim Cosmochim Acta, 182, 55-72.

Meng, M., R. Sun, H. Liou, B. Yu, Y. Yin, L. Hu, J. Chen, J. Shi, and G. Jiang (2020), Mercury isotope variations within the marine food web of Chinese Bohai Sea: Implications for mercury sources and biogeochemical cycling, J. of Haz. Mat., 384, 121379.

Meng, M., R. Y. Sun, H. W. Liu, B. Yu, Y. G. Yin, L. G. Hu, J. B. Shi, and G. B. Jiang (2019), An integrated model for input and migration of mercury in Chinese coastal sediments, Environ. Sci. Technol., 53, 2460-2471.

Moynier, F., J. Chen, K. Zhang, H. Cai, Z. Wang, M. G. Jackson, and J. Day (2020), Chondritic mercury isotopic composition of Earth and evidence for evaporative equilibrium degassing during the formation of eucrites, Earth Planet. Sci. Lett., 551, 116544.

Mukhopadhyay, S., and R. Parai (2019), Noble Gases: A Record of Earth's Evolution and Mantle Dynamics, Annual Rev. Earth Planet. Sci. , 47, 389-419.

Mundl-Petermeier, A., R. J. Walker, R. A. Fischer, V. Lekic, M. Jackson, and M. Kurz (2020), Anomalous 182W in high $^{3}He/^{4}He$ ocean island basalts: fingerprints of Earth's core?, Geochim. Cosmochim. Acta 194–211.

Óskarsson, N., Sigvaldason, G.E., and Steinthorsson, S., 1982, A dynamic-model of rift-zone petrogenesis and the regional petrology of Iceland: Journal of Petrology, v. 23, p. 28–74, doi: 10 .1093 /petrology /23 .1 .28.

Peters, B. J., R. Carlson, J. M. D. Day, and M. F. Horan (2018), Hadean silicate differentiation preserved by anomalous $^{142}Nd/^{144}Nd$ ratios in the Réunion hotspot source., 555, 89-93.

Pik, R., B. Marty, and D. Hilton (2006), How many mantle plumes in Africa? The geochemical point of view, Chem. Geol., 226, 100-114.

Rasmussen, M. B., S. A. Halldórsson, S. A. Gibson, and G. H. Guðfinnsson (2019), Olivine chemistry reveals compositional source heterogeneities within a tilted mantle plume beneath Iceland, Earth Planet. Sci. Lett., 531, 116008.

Rizo, H., D. Andrault, N. Bennet, M. Humayun, A. Brandon, I. Vlastelic, B. Moine, A. Poirier, M. Bouhifd, and D. Murphy (2019), $^{182}W$ evidence for core-mantle interaction in the source of mantle plumes., Geochem. Perspect. Lett. , 11, 6-11.

Sherman, L., J. Blum, K. Johnson, G. Keeler, J. Barres, and T. Douglas (2010), Mass-independent fractionation
of mercury isotopes in Arctic snow driven by sunlight, Nat. Geosci., 3, 173-177.

Sonke, J., J. Schafer, J. Chmeleff, S. Audry, G. Blanc, and B. Dupre (2010), Sedimentary mercury stable isotope
records of atmospheric and riverine pollution from two major European heavy metal refineries, Chem. Geol., 279, 90-100.

Stracke, A. (2012), Earth's heterogeneous mantle: A product of convection-driven interaction betweencrust and mantle, Chem. Geol., 330, 274-299.

Varas-Reus, M. I., S. Konig, A. Yierpan, J. P. Lorand, and R. Schoenberg (2019), Selenium isotopes as tracers of a late volatile contribution to Earth from the outer Solar System, Nature Geosci., 12, 779–782.

Wang, Z. Z., and H. Becker (2013), Ratios of S, Se and Te in the silicate Earth require a volatile-rich late veneer, Nature, 499, 328-331.

White, W. (2015), Isotopes, DUPAL, LLSVPs, and Anekantavada., Chem. Geol., 419, 10–28.

White, W. M., and A. W. Hofmann (1982), Sr and Nd isotope geochemistry of oceanic basalts and mantle evolution, Nature, 296, 821-825.

Workman, R. K., S. Hart, J. Eiler, and M. Jackson (2008), Oxygen isotopes in Samoan lavas: confirmation of continent recycling, Geology, 36, 551-554.
Yin, R. S., X. B. Feng, B. Chen, J. Zheng, W. Wang, and X. Li (2015), Identifying the source and processes of mercury in subtropical estuarine and ocean sediments using Hg isotopic composition., Environ. Sci. Tech., 49, 1347-1355.
Yuan, S., J. Chen, H. Cai, W. Yuan, Z. Wang, Q. Huang, Y. Liu, and X. Wu (2018), Sequential samples reveal significant variation of mercury isotope ratios during single rainfall events., Sci. Total Environ., 624, 133-144.
Zambardi, T., J. Sonke, J.-P. Toutain, F. Sortnob, and H. Shinoharac (2009), Mercury emissions and stable isotopic compositions at Vulcano Island (Italy), Earth Planet. Sci. Lett., 277, 236-243.
Zhang, Y., et al. (2020), Mercury isotope compositions in large anthropogenically impacted Pearl River, South China., Ecotox. Environ. Safety, 191, 110229.
Zindler, A. W., and S. R. Hart (1986), Chemical Geodynamics, Ann. Rev. Earth Planet. Sci., 14, 493-571.

## References From the Supporting Information

Jackson, M., S. R. Hart, A. Koppers, H. Staudigel, J. Konter, J. Blusztajn, M. Kurz, and J. Russell (2007), The return of subducted continental crust in Samoan lavas, Nature 448, 684-687.
Jackson, M. G., et al. (2020), Ancient He and W isotopic signatures preserved in mantle domains least modified by crustal recycling, PNAS, 117, 30993-31001.
Macpherson, C. C., D. Hilton, J. Day, D. Lowry, and K. Gronvold (2005), High-3He/4He, depleted mantle and low d18O, recycled oceanic lithosphere in the source of central Iceland magmatism, Earth Planet. Sci. Lett., 233, 411–427
Füri, E., D. Hilton, S. Halldórsson, P. Barry, D. Hahm, T. Fischer, and K. Grönvold (2010), Apparent decoupling of the He and Ne isotope systematics of the Icelandic mantle: The role of He depletion, melt mixing, degassing fractionation and air interaction, Geochim. Cosmochim. Acta, 74, 3307–3332.
Garapic, G., M. Jackson, E. Hauri, S. R. Hart, K. A. Farley, J. Blusztajn, and J. Woodhead (2015), A radiogenic isotopic (He-Sr-Nd-Pb-Os) study of lavas from the Pitcairn hotspot: Implications for the origin of EM-1 (enriched mantle 1), Lithos, 228, 1-11.

Figure Caption:

Figure 1: $\Delta^{199}$Hg versus $\delta^{202}$Hg for all samples analyzed here. Samples from the Afar, Ofu island, and Iceland have similar $\Delta^{199}$Hg that cluster around zero and variable $\delta^{202}$Hg values. A sample from Tubuai has a positive $\Delta^{199}$Hg value, whereas two Pitcairn samples and one Samoan sample with recycling signatures have negative $\Delta^{199}$Hg.

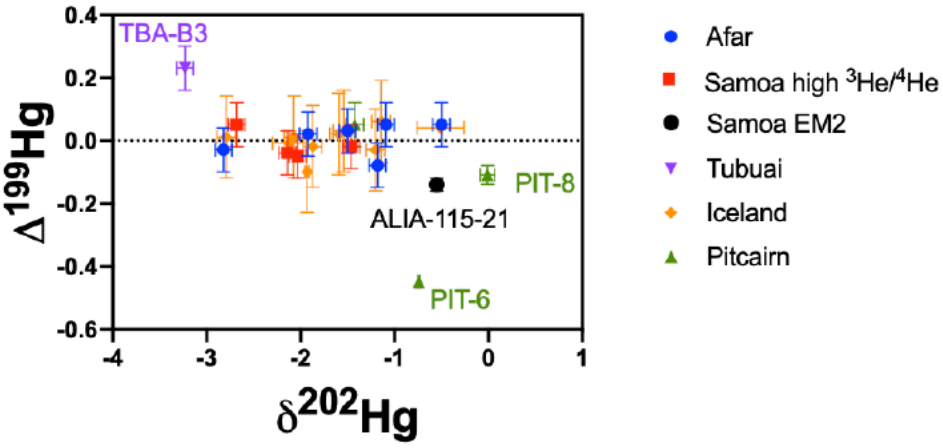

548 Figure 2: $^{87}Sr/^{86}Sr$ versus $\Delta^{199}Hg$ for Pitcairn lavas. The correlation of $\Delta^{199}Hg$ values with $^{87}Sr/^{86}Sr$ suggests a
549 mixture of both recycled oceanic crust (high $^{87}Sr/^{86}Sr$ and $\Delta^{199}Hg$) and terrigenous materials (low $^{87}Sr/^{86}Sr$ and
550 $\Delta^{199}Hg$) in the Pitcairn mantle source. $^{87}Sr/^{86}Sr$ data from Garapic et al. [2015].
551

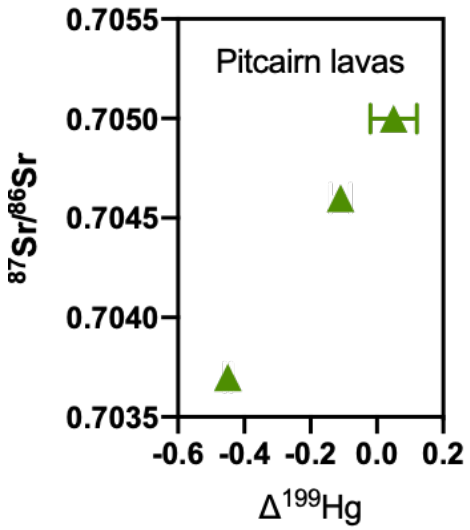


552
553
554
555
556
557
558
559
560
561
562
563
564
565
566
567

568 Figure 3: Mercury isotopic composition of the Earth's mantle (red box, defined by high $^{3}He/^{4}He$ lavas from Samoa
569 and Iceland) compared to chondrites (CC=carbonaceous chondrites, EC=enstatite chondrites, OC=ordinary
570 chondrites). Mantle-derived lavas exhibit no clear signatures for crustal recycling and fall within the chondritic
571 range..
572

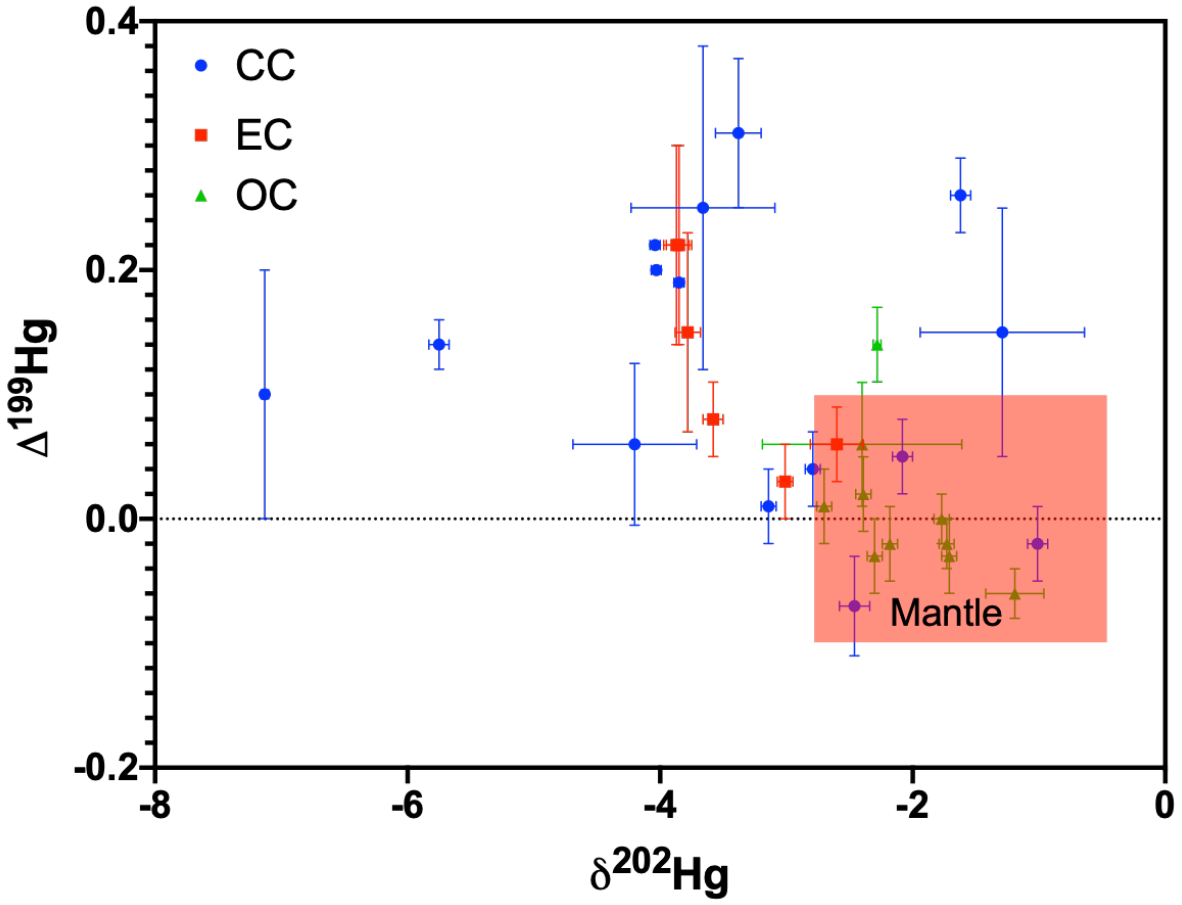


573
574
575
576
577
578
579
580

Figure 4: $\Delta^{199}$Hg versus $\Delta^{201}$Hg for the Earth's mantle (red box, defined by high $^{3}$He/$^{4}$He lavas from Samoa and Iceland), Pitcairn, Tubuai and Samoa lavas. HIMU (Tubuai), EM-1 (Pitcairn) and EM-2 (Samoa) deviates from the mantle composition, reflecting a contribution of recycled surface materials in their mantle sources (marine material for Tubuai, continental material for Samoa, and both marine and continental material in the Pitcairn mantle).

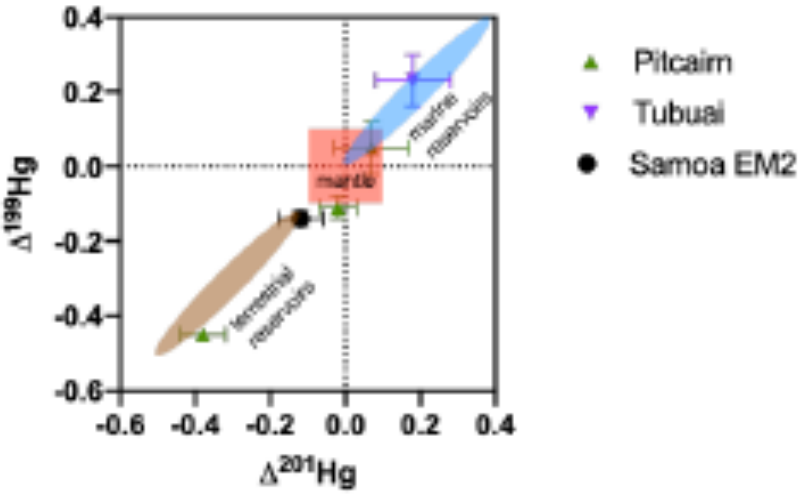

601 Table S1

602 **Introduction** This table contains the mercury isotopic composition the samples analysed in this study. The full data
603 table can be found in supplementary materials (Table S1) and the Figure S1 (our Hg isotope data plotted against Nd
604 isotope ratios). Helium isotopic data are from [*Jackson et al.*, 2007; *Jackson et al.*, 2020; *Macpherson et al.*, 2005;
605 *Furi et al.* 2010]. All the data were collected in 2021 on a Nu Instruments Multi-collectors inductively-coupled-
606 plasma mass-spectrometer.

607

608
609
610
611
612 **Table S1:**
613

| Samples | $\delta^{202}$Hg | 2SD | $\Delta^{199}$Hg | 2SD | $\Delta^{200}$Hg | 2SD | $\Delta^{201}$Hg | 2SD | $\Delta^{204}$Hg | 2SD | $^{3}$He/$^{4}$He (Ra) |
|---|---|---|---|---|---|---|---|---|---|---|---|
| **Afar** | | | | | | | | | | | |
| AF13-339 | -0.50 | 0.09 | 0.05 | 0.07 | 0.05 | 0.07 | 0.08 | 0.10 | -0.02 | 0.18 | |
| AF13-356 | -1.50 | 0.09 | 0.03 | 0.07 | 0.01 | 0.07 | -0.02 | 0.10 | -0.07 | 0.18 | |
| AF13-44 | -1.09 | 0.09 | 0.05 | 0.07 | 0.03 | 0.07 | 0.05 | 0.10 | -0.03 | 0.18 | |
| AF13-48 | -1.92 | 0.09 | 0.02 | 0.07 | 0.02 | 0.07 | 0.06 | 0.10 | -0.11 | 0.18 | |
| AF13-56 | -1.18 | 0.09 | -0.08 | 0.07 | -0.07 | 0.07 | 0.01 | 0.10 | -0.02 | 0.18 | |
| AF13-90 | -2.82 | 0.09 | -0.03 | 0.07 | 0.09 | 0.07 | 0.05 | 0.10 | -0.05 | 0.18 | |
| **Samoa** | | | | | | | | | | | |
| ALIA-115-21 | -0.55 | 0.03 | -0.14 | 0.02 | 0.02 | 0.02 | -0.12 | 0.06 | -0.04 | 0.07 | |
| Ofu-04-03 | -2.03 | 0.09 | -0.05 | 0.07 | -0.02 | 0.07 | -0.03 | 0.10 | 0.03 | 0.18 | 24 |
| Ofu-04-06 | -2.68 | 0.09 | 0.05 | 0.07 | 0.10 | 0.07 | -0.07 | 0.10 | -0.02 | 0.18 | 34 |
| Ofu-04-10 | -2.14 | 0.09 | -0.04 | 0.07 | 0.01 | 0.07 | -0.07 | 0.10 | -0.22 | 0.18 | 22 |
| Ofu-04-15 | -1.46 | 0.09 | -0.02 | 0.07 | 0.01 | 0.07 | -0.03 | 0.10 | -0.02 | 0.18 | 30 |
| **Pitcairn** | | | | | | | | | | | |
| PIT-13 | -1.42 | 0.09 | 0.05 | 0.07 | 0.05 | 0.07 | 0.07 | 0.10 | 0.00 | 0.18 | 9 |
| PIT-6 | -0.74 | 0.01 | -0.45 | 0.01 | -0.01 | 0.05 | -0.38 | 0.06 | 0.05 | 0.05 | |
| PIT-8 | -0.01 | 0.08 | -0.11 | 0.03 | 0.03 | 0.03 | -0.02 | 0.05 | -0.03 | 0.09 | 8 |
| **Tubuai** | | | | | | | | | | | |
| TBA-B3 | -3.23 | 0.09 | 0.23 | 0.07 | 0.04 | 0.07 | 0.18 | 0.10 | -0.10 | 0.18 | 7 |
| **Iceland** | | | | | | | | | | | |
| *Eastern Rift Zone* | | | | | | | | | | | |
| A11 | -0.51 | 0.25 | 0.04 | 0.01 | 0.00 | 0.02 | -0.01 | 0.10 | 0.00 | 0.25 | 24 |
| A24 | -2.07 | 0.10 | 0.01 | 0.13 | 0.03 | 0.08 | 0.01 | 0.10 | -0.16 | 0.25 | 26 |
| *Reykjanes Peninsula and Western Rift Zone* | | | | | | | | | | | |
| STAP-1 | -1.87 | 0.10 | -0.02 | 0.13 | 0.02 | 0.08 | 0.01 | 0.10 | -0.01 | 0.25 | 14 |
| VIF-1 | -1.59 | 0.10 | 0.02 | 0.13 | 0.07 | 0.08 | 0.06 | 0.10 | -0.10 | 0.25 | 13 |

| | | | | | | | | | | | |
|---|---|---|---|---|---|---|---|---|---|---|---|
| MID-1 | -1.54 | 0.11 | 0.03 | 0.13 | 0.05 | 0.08 | 0.02 | 0.16 | 0.17 | 0.07 | 17 |
| *Northern Rift Zone* | | | | | | | | | | | |
| NAL-625 | -1.93 | 0.02 | -0.10 | 0.13 | 0.06 | 0.03 | -0.08 | 0.02 | 0.03 | 0.03 | 34 |
| *South Iceland Volcanic Zone* | | | | | | | | | | | |
| SAL-601 | -1.14 | 0.10 | 0.06 | 0.13 | 0.06 | 0.08 | 0.01 | 0.10 | 0.04 | 0.25 | 19 |
| **Geostandards** | | | | | | | | | | | |
| BCR-2 | -2.18 | 0.09 | -0.01 | 0.07 | 0.02 | 0.07 | 0.00 | 0.10 | 0.02 | 0.18 | |
| BCR-2 (Geng et al.) | -2.08 | 0.08 | 0.00 | 0.14 | 0.01 | 0.08 | 0.00 | 0.14 | | | |
| RGM-2 | -0.98 | 0.09 | -0.02 | 0.07 | 0.02 | 0.07 | -0.03 | 0.10 | 0.02 | 0.18 | |
| STM-2 | -1.11 | 0.09 | 0.00 | 0.07 | 0.01 | 0.07 | -0.01 | 0.10 | -0.12 | 0.18 | |
| BE-N | -3.08 | 0.08 | 0 | 0.03 | 0.01 | 0.03 | -0.02 | 0.05 | -0.01 | 0.09 | |
| *UoI internal standards* | | | | | | | | | | | |
| I-ICE | -2.12 | 0.18 | -0.01 | 0.04 | 0.01 | 0.03 | -0.04 | 0.02 | 0.00 | 0.10 | |
| A-ALK | -1.20 | 0.10 | -0.03 | 0.13 | -0.02 | 0.08 | -0.06 | 0.10 | 0.00 | 0.25 | |
| B-ALK | -2.79 | 0.10 | 0.01 | 0.13 | 0.08 | 0.08 | -0.03 | 0.10 | -0.01 | 0.25 | |

References:

Jackson, M., S. R. Hart, A. Koppers, H. Staudigel, J. Konter, J. Blusztajn, M. Kurz, and J. Russell (2007), The return of subducted continental crust in Samoan lavas, *Nature 448*, 684-687.

Jackson, M. G., et al. (2020), Ancient He and W isotopic signatures preserved in mantle domains least modified by crustal recycling, *PNAS*, *117*, 30993-31001.

Macpherson, C. C., D. Hilton, J. Day, D. Lowry, and K. Gronvold (2005), High-3He/4He, depleted mantle and low d18O, recycled oceanic lithosphere in the source of central Iceland magmatism, *Earth Planet. Sci. Lett.*, *233*, 411–427

Füri, E., D. Hilton, S. Halldórsson, P. Barry, D. Hahm, T. Fischer, and K. Grönvold (2010), Apparent decoupling of the He and Ne isotope systematics of the Icelandic mantle: The role of He depletion, melt mixing, degassing fractionation and air interaction, Geochim. Cosmochim. Acta, 74, 3307–3332.